

DEVELOPMENT OF AN IN-VESSEL SEVERE ACCIDENT ANALYSIS CODE MIDAC

Longze Li, Yapei Zhang, Wenxi Tian, G. H. Su*, Suizheng Qiu, Ronghua Chen

Department of Nuclear Science and Technology, Xi'an Jiaotong University
Xi'an 710049, China

lilongze.89@hotmail.com; zhangyapei@mail.xjtu.edu.cn; wxtian@mail.xjtu.edu.cn;
ghsu@mail.xjtu.edu.cn; szqiu@mail.xjtu.edu.cn; rhchen@mail.xjtu.edu.cn;

ABSTRACT

The Module In-vessel Degradation severe accident Analysis Code (MIDAC) is developed by Xi'an Jiaotong University to meet the domestic demand of software autonomous scheduling. The whole processes of in-vessel severe accident can be analyzed by the code with credible results. The code is composed of five main modules: the core early behavior module, the core degradation module, the debris bed module, the RPV melt behavior module and the thermal hydraulic module. These modules are combined with each other and can simulate almost all the severe accident phenomena in the vessel. The core early behavior module contains models for phenomena as the core heat up after the core exposure, the cladding oxidation reaction, the cladding ballooning, the fuel-cladding interaction and other related phenomena. Core degradation module can calculate the core melt and relocation process in the core. A new candling model is developed to determine the behavior of melting material outside the fuel rods, including the melt flow and freeze. The debris bed module can be used to analyze the process of the formation and cooling of the debris both in the core and lower plenum. RPV melt behavior module treats the heat transfer of the corium pool to the lower head and determines the property of the in-vessel retention of the corium. The thermal hydraulic module is well developed to interact with all the other modules and combine them to a uniform MIDAC code. A preliminary validation of the code with TMI-2 accident has already been done and the simulation results show good agreement with the real plant data.

KEYWORDS

MIDAC, in-vessel, severe accident, modules

1. INTRODUCTION

The severe accident is a kind of beyond design basis accidents (BDBAs) in which core damage could occur, jeopardizing both the economy and the environment. The research of nuclear power plant (NPP) accident was started at 1950s, even before the building of the first truly commercial NPP [1]. However, only until the TMI-2 accident [2] at 1979 that the probability of severe accident in NPP was accepted all over the world. Immediately after this accident, both the experimental and analysis development research programs were initiated to investigate the progression and consequences of severe accidents, not only in United States, but also in European countries [3]. The Chernobyl accident, happened in 1986, provided the public with a vivid demonstration of the hazard of the core-melt accident and the poor knowledge of the severe accident. The TMI-2 accident and Chernobyl accident created difficult years for the nuclear industry, as well as the boom of SA research. The Chinese commercial nuclear power plant development accelerated since the 1990s, and the relevant NPP accident research was mostly limited on the design basis accidents, causing the shortage of severe accident research in China. Things just changed in 2011,

when the Fukushima accident happened in Japan. It reminds the Chinese government the nuclear safety of the NPP in China, attracting more attention to the severe accident research.

The demands for acceptance of nuclear power demand full deterministic evidence of NPP safety. Thus, the severe accident codes which provide precise deterministic analysis of NPP safety are significant to the existing and the next generation of NPPs [4]. Nowadays, generally three classes of SA codes can be defined, according to their scope of application: integral codes, detailed codes, and dedicated codes [1]. The integral codes, also called the engineering-level codes, can simulate almost all the nuclear power plant response with the relatively rough models. The principal internationally used integral codes today are MAAP, MELCOR, and ASTEC. The detailed codes are characterized by best-estimate phenomenological models, consistent with the state of the art, to enable, as far as possible, an accurate simulation of the behavior of a nuclear power plant in severe accident. The principal internationally used codes today are ATHLET-CD, SCDAP/RELAP5, and ICARE/CATHARE. The dedicated codes aim at simulating a single phenomenon, like the MC3D and TEXAS for steam explosion phenomenon and CORCON for molten corium concrete interaction (MCCI) phenomenon.

Although the research on SA codes development in China was in a primary level which can't meet the need of rapid development in the nuclear industry, some Chinese researchers' efforts on this area should be admitted. Currently, Xi'an Jiaotong University has developed several dedicated severe accident analysis codes aiming on the single phenomena, such as the core oxidation [5], the debris bed [6, 7] the molten materials in-vessel retention (IVR) [8], the FCI [9], the core reflooding, the MCCI and the hydrogen burning. The researchers in Xi'an Jiaotong University also have plenty experience in simulating the NPP severe accident with integral SA codes like MAAP [10, 11, 12] and MELCOR [13].

The Module In-vessel Degradation severe accident Analysis Code (MIDAC) code is developed by Xi'an Jiaotong University based on the SA research experience to meet the domestic demand of software autonomous scheduling. The code focuses on the phenomena during the in-vessel severe accident processes, such as the core heat-up, core oxidation, cladding ballooning, core material eutectic interaction, core melting and relocation, debris bed formation and heat transfer, and corium in-vessel retention. The advanced models developed in the recent severe accident study as well as many verified models in the existing SA code as MAAP, MELCOR and SCDAP are added to some of the physical models in the code which provide a more reliable simulation result of the code. A visual interface program is going on designed for a better human and computer interaction (HCI). The code is developed as a domestic tool of which the simulation results are meaningful for making of the severe accident EOPs and SAMG. In this work, the main structure and physical models are introduced, and the preliminary code validation with TMI-2 accident data is given.

2. Mathematic and physical models of MIDAC

The MIDAC code is composed of five main modules as shown in Fig. 1: the core early behavior module, the core degradation module, the debris bed module, the RPV melt behavior module and the thermal hydraulic module. These modules are combined with each other and can simulate almost all the severe accident phenomena in the vessel. The former four modules corresponding to the four phases of in-vessel severe accident and the thermal hydraulic module is well developed to interact with all the other modules and combine them to a uniform MIDAC code. The selected mathematic and physical models in former four severe accident process modules are introduced in this part due to space limitations. The relevant work will be presented in detail in the article which describes the corresponding module of MIDAC.

2.1. The core early behavior module

The core early behavior module describes the mechanism and phenomena in early phase of in vessel severe accident. Important phenomena includes the core heat-up after the exposure, the zircaloy and steel oxidation in the cladding or other core structures, the cladding ballooning and rupture, fuel-cladding interaction and some other thermal hydraulic phenomena. The zircaloy oxidation which mainly caused by

Zr-water reaction and the Zr-air reaction is important to the accident. The two reactions have great influence on the sequence [14] and are introduced to represent for early behavior module. The chemical equation of Zr-water reaction is shown below:

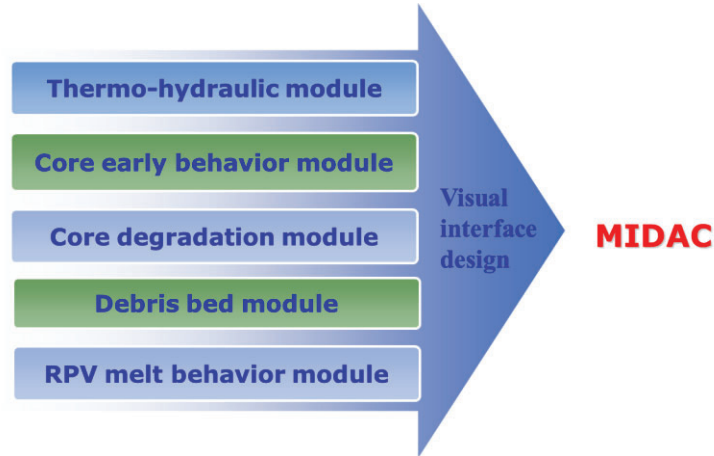


Figure 1. Structure of MIDAC



Where ΔH_{Zr} is the reaction heat per mole of Zr consumed, with the value of $6.16 \times 10^8 \text{ J}/(\text{kg}\cdot\text{mol})$ herein. This oxidation is assumed to take place at the interface of zircaloy and ZrO_2 in MIDAC code, leading to the growth of the oxide layer. The kinetics of the reaction rate is reflected by the parabolic correlations according to the experiments [15, 16]. The MIDAC code provides several choices of the parabolic correlations which are used in other SA codes or verified in the public literature for the user. A new model which combined the Cathcart-Pawel correlation [15] for the low temperature and so called best-fitted correlation [17] for the high temperature is presented herein. The model is based on hydrogen measurements which include total oxygen uptake to form ZrO_2 and $\alpha\text{-ZrO}_2$. The equivalent rate-of-change of a single ZrO_2 layer is:

$$\dot{x} = \begin{cases} \frac{294}{2\rho_{\text{Zr}}^2 x} e^{-1.671 \cdot 10^8 / RT} & T \leq 1800\text{K} \\ \frac{22787}{2\rho_{\text{Zr}}^2 x} e^{-2.230 \cdot 10^8 / RT} & T \geq 1900\text{K} \\ \frac{22787}{2\rho_{\text{Zr}}^2 x} e^{\left[-2.230 \cdot 10^8 / RT - 7.10 \cdot 10^8 \left(1/T - 1/1900^2 \right) \right]} & 1800\text{K} \leq T \leq 1900\text{K} \end{cases} \quad (2)$$

Where T is the temperature of cladding or other zircaloy core structures, x is the equivalent oxide thickness, including ZrO_2 and effective $\alpha\text{-ZrO}_2$ layers, ρ_{Zr} is the density of Zr, R is the ideal gas constant ($8.314 \text{ kJ}/(\text{kg}\cdot\text{mol}\cdot\text{K})$).

The consequence of air ingress to the reactor pressure vessel (RPV) would become a huge concern since the Zr-air reaction is even more exothermic than the Zr-water reaction. Nitrogen may also diffuse into the zircaloy, especially when the oxygen is used up. A parabolic correlation is implemented for the

oxide layer growth rate in the code for consistency. The equivalent rate-of-change of a single ZrO₂ layer is [18]:

$$\dot{x} = \begin{cases} \frac{10.50}{2\rho_{Zr}^2 x} e^{-15630/T} & T < 1333K \\ \frac{2.511 \times 10^5}{2\rho_{Zr}^2 x} e^{-28485/T} & 1333K \leq T \leq 1550K \\ \frac{50.40}{2\rho_{Zr}^2 x} e^{-14634/T} & T > 1550K \end{cases} \quad (3)$$

A mechanism model to calculate the cladding strain and deformation which take the circular, axial and radial stress into consideration is developed and implemented into the cladding ballooning model in the early behavior module. Other models as the oxidation of stainless steel, the fuel-cladding interaction and etc. are also taken into account in the module.

2.2. The core degradation module

Core degradation module can calculate the core melt and relocation process in the core. The core melt and initial relocation encompasses low-temperature material interaction, metallic and U-Zr-O type melt formation and relocation. The core melt is usually started with dissolution or eutectic reactions of core materials at temperatures much below the melting temperatures of the fuel and its cladding. These reactions involve control rods, fuel rods, and other core structural materials, forming relatively low temperature liquid phases [14]. With the core temperature increasing, core materials melt accelerates especially when the temperature reaches the melting point. These melting materials flow downwards in the core until reaching cooler regions where the materials tend to solidify, forming blockages in the flow channels between fuel rods. This process is vividly called the candlering. The blockages can restrict flow area of the core and deteriorate heat-up of the core. As a result of diversion of steam around the blockages and their low thermal conductivity, heat transfer from the blockage is slow, and a molten pool can form. Once formed, the molten pool with the ceramic crust in the core is difficult to cooling down, and has great influence on the core melting process in the other parts of core with rod-like geometry. The core reflooding phenomenon that may exist in the core early phase or core degradation phase of the severe accident is also considered. The core reflooding may cool down the core region when the core remains the rod like geometry while may fail to do that once the molten pool with ceramic crust formed as in TMI-2 accident.

A new candlering model is developed in MIDAC to determine the behavior of melting material outside the fuel rods, and this model is introduced here to represent the complex models in the core degradation module. In the candlering process, three main parameters should be calculated: melting material moving down, melting material solidification after moving, remaining melting material after moving. In this article, only the model of calculating melting material moving down is presented. The model has two kind of flow mechanisms based on the outer membrane flow and internal tubular flow respectively. When fuel rods don't contact with each other (i.e., their gaps are greater than their diameters), outer membrane flow (or film flow) regime will take place, which is showed in Fig. 2. Besides, the internal tubular flow (or pipe flow) may be better when considering the inside situation. If membrane flow takes place, the thickness of stable film on cylindrical fuel rod of donor node is:

$$\delta = \frac{m_p}{N\rho XL_D} \quad (4)$$

Where m_p is the mass of core melting materials of donor node with density ρ , X is a kind of perimeter defined as $X=4A/D_h$, L_D is length of the donor node, A is the flow area in the core, D_h is the hydraulic diameter, and N is the number of rods in the donor node. When stable film flow formed, the gravity and viscosity force is equal, and the relation between average velocity and thickness of film is:

$$U_f = \frac{\rho g}{3\mu} \delta^2 \quad (5)$$

Where μ is dynamic viscosity of melting materials, g is acceleration of gravity. The rate of stable film flow can be calculated as:

$$W_f = \rho \delta U_f X N \quad (6)$$

The membrane flow may transfer to the internal tubular flow once the nodes are restricted by the blockage and drainage of the melt from the donor nodes become limited by the flow through very small passages. The rate of internal flow can be approximated as:

$$W_p = \frac{-B + \sqrt{B^2 - 4C}}{2} \quad (7)$$

$$B = 64 \cdot \mu A_p L / (D_h)^2$$

$$C = (\rho A_p)^2 (2g \cdot h)$$

Where A_p is the internal flow area in the receiving node, L is the axial length in receiving node, h is the driving head.

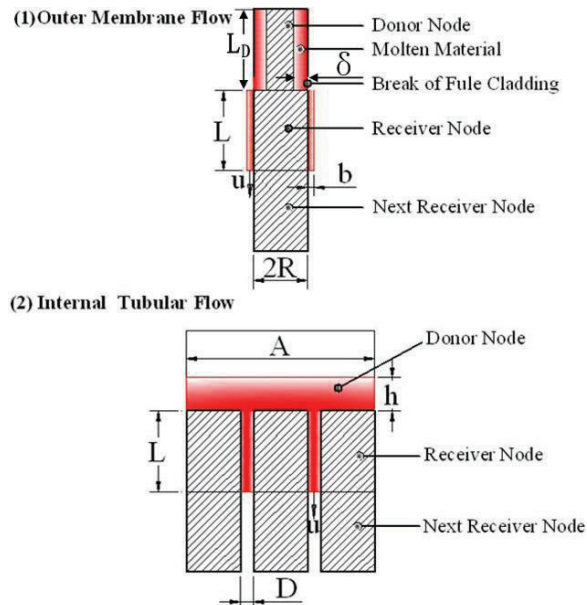


Figure 2. Downward Flow Mechanisms.

2.3. The debris bed module

The debris bed module can be used to analyze the process of the formation and cooling of the debris in lower plenum. The molten materials in the core can relocate to the lower plenum. Three relocation scenarios in the lower plenum are possible in MIDAC code: lateral crust failure and relocation via the core pass, bottom crust failure and jet flow through the lower support plate, and massive relocation due to failure of lower support plate.

If water pool existed in the lower plenum, as in most accident sceneries, core debris breakup and fragmentation due to interaction with the pool, or the fuel coolant interaction (FCI) is modeled in MIDAC code. In general, during a hypothetical severe accident, the penetration of molten corium into the water of the low plenum or cavity [19] will lead to the appearance of porous debris [20, 21]. Once the debris settles down at the lower plenum, two types of debris behavior, ie., the particulate debris bed and continuum bed, are considered. Newly developed three layer (metal layer, debris pool, and heavy metal layer) lower plenum corium pool model is implemented into the debris bed model to consider the influence of the so-called “heavy metal” layer in the continuum bed. The structure of the debris bed in lower plenum is depicted in Fig.3. The un-oxidized Zr in corium pool can react with UO₂ to produce U metal, and the heavy metal layer separate from the oxidic molten corium pool which is comprised of mixture of U, Zr, steel and oxygen. The model is based on the simplified U-Zr-steel-O phase diagram and the approach proposed by Salay and Fichot [22]. The mole fractions in the oxidic melt and heavy metal are defined as:

$$F_{OXI} = \frac{\frac{m_{U1}}{238} + \frac{m_{Zr1}}{91.22} + \frac{m_{O1}}{16.0} + \frac{m_{S1}}{55.85}}{\frac{m_{U0}}{238} + \frac{m_{Zr0}}{91.22} + \frac{m_{O0}}{16.0} + \frac{m_{S0}}{55.85}} = \frac{x_1 - x_0}{x_1 - x_2} \quad (8)$$

$$F_{HM} = \frac{\frac{m_{U2}}{238} + \frac{m_{Zr2}}{91.22} + \frac{m_{O2}}{16.0} + \frac{m_{S2}}{55.85}}{\frac{m_{U0}}{238} + \frac{m_{Zr0}}{91.22} + \frac{m_{O0}}{16.0} + \frac{m_{S0}}{55.85}} = \frac{x_0 - x_2}{x_1 - x_2} \quad (9)$$

Where where F_{OXI} and F_{HM} are mole fractions in the oxidic melt and heavy metal respectively, the m terms are the masses of constituents in the oxidic melt (subscript 1), the heavy metal (subscript 2) and total corium (subscript 0). x_0 , x_1 , and x_2 are mole fraction already been obtained from the phase diagram of U-Zr-Steel-O system.

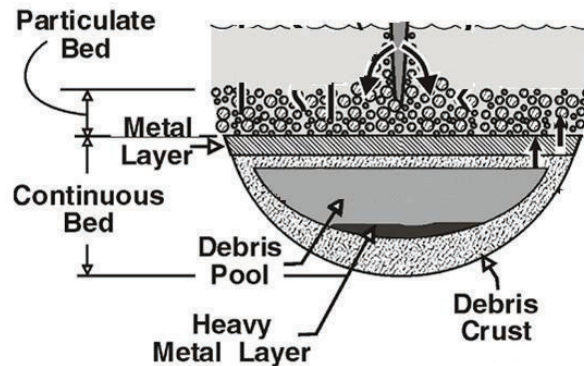


Figure 3. Structure of Debris Bed in Lower Plenum

2.4. RPV melt behavior module

RPV melt behavior module treats the heat transfer of the corium pool to the lower head and determines the property of the in-vessel retention of the corium. The long-term behavior of corium pool in the lower plenum is important for the estimation of RPV failure and the IVR property. If sufficient water is available and the accumulated melt mass in the lower plenum limited as in TMI-2, then a water-filled gap between the crusted melt and the RPV wall might protect the wall from thermal loads. The estimation of the RPV failure is mainly determined by the factors as the corium melt mass accumulated, the heat flux distribution, the melting of structure material in the lower plenum, and the local or global failure mode of the RPV wall.

Five RPV failure mechanisms are considered in MIDAC code: molten core debris attack on lower head may result in the failure of penetration, heating from accumulated debris may lead to ejection of the penetration, high pressure and temperature can cause the creep rupture of the RPV, debris jet directly onto the lower head can lead to localized ablation of lower head, the molten metal layer on top of the corium pool can thermally attack and weaken the vessel wall.

3. VALIDATION OF MIDAC CODE

3.1. Validation matrix

The code assessment is important to ensure the reliability of the code which consisted of two stages, called the “verification” and “validation”. The verification mainly involved the code specification and coding, the accuracy of the code solution and so on. The validation aims at demonstrating the physics models, mainly by comparing the code results with results of experimental programs. A preliminary validation matrix is defined in this work based on the severe accident experimental research [23] as shown in Table I. A set of experiments, for which comparison of the measured and calculated parameters forms the basis for establishing the accuracy of test predictions, is included in this matrix. The experiments are all integral tests currently, which cover almost all the in-vessel severe accident thermal hydraulic phenomena expected in light water reactor.

The TMI-2 was an accident at full scale, with insights into the behavior of a plant during all stages of an in vessel severe accident sequence. It has been very extensively documented and analyzed. However, the available measurements from TMI-2 were insufficient to provide information about progression of the accident. The chief value of TMI-2 is its uniqueness in terms of scale and range of phenomena encountered.

The CORA-7 and CORA-13 provides well-qualified, well-documented and extensively analyzed data on an electrically heated PWR bundle quenched during early phase melt progression. Phebus FP project consists of a set of experiments to investigate severe fuel damage and source term release on a reduced scale, using fuel irradiated to prototypical reactor levels. PBF-SFD test is also an “in-reactor” core degradation test using fission power and decay power to provide the intended thermal power and irradiation boundary. Quench-06 test was used as an OECD International Standard Problem (ISP-45) which investigated the behavior of pre-oxidized fuel rods reflooded from the bottom of the bundle.

Table I. The preliminary validation matrix of MIDAC

Program name	Organization
TMI-2 accident	--
CORA-7	KIT(Germany)
CORA-13	KIT(Germany)

PHEBUS FPT1	IRSN(France)
PBF-SFD Test 1-4	INEL(US)
QUENCH-06	KIT(Germany)

3.2. Validation on TMI-2 accident

The TMI-2 accident can be generally divided into five distinct phases [24]. Phase 1(0-100 min) is a small loss of coolant accident (LOCA) with some or all of the main coolant pump (MCP) were operating. Phase 2 (100-174 min) represents the part of accident where all coolant pumps were shut down and resulted in the core uncovering, heat-up and damage. Phase 3 (174-224 min) begins with the restart of reactor coolant pump 2B. Coolant injected cooled the peripheral fuel assemblies while core heat-up and damage continued, forming a debris bed in the upper core region. Phase 4 (224-235 min) is characterized by the core material relocating into the lower head through the side crust of the molten pool. In Phase 5 (235-300 min), the debris in the lower plenum caused the RPV wall temperature to increase to about 1100 °C and then the wall was rapidly cooled. The MIDAC code was used to simulate all five phases of the TMI-2 accident. The TMI-2 plant geometry, operator performance, controls and initial conditions plant data are covered as input data for MIDAC simulation, parts of the initial state of the TMI-2 plant are list in the Table I.

Table II. The initial state of the TMI-2 plant

Parameter	TMI-2 Design Value	MIDAC Steady Value
Thermal power,MW	2272	2272
Primary pressure,MPa	15.0	14.92Mpa
Secondary pressure, MPa	6.895	6.5
Average core coolant temperature, K	579.15	578.8
Flow rate in each loop, kg/s	8500	8515

The TMI-2 accident data and MIDAC calculating results are compared in this section. The RCS pressure is depicted in Fig. 4. It is shown that the MIDAC result agrees well with the TMI-2 data in term of the whole variation trends. The pressure was well predicted before the loop B MCP stop, and was over-predicted soon after that. The pressure increased after the MCP stop and the worse cooling of the steam generator (SG) secondary side, until the loop A MCP stop. Pressure peak emerged in MIDAC calculation was bigger than the data. The pressure decreased faster after that, leading to the lower-prediction of the pressure, especially in the lowest point of the curve. The pressure increased after the pilot-operated relief valve (PORV) closed by the operator in 142 min, and was well agreed with the TMI-2 data. The maximum value of pressure was slightly over predicted at about 180min. At 174min, the MCP in loop B was restarted by the operator, pumping about 30 m³ coolant into the reactor vessel. The consequent water vaporization in the lower plenum resulted in pressure increase. The RCS pressure then decrease, and the high pressure injection at about 200 min accelerated this decrease. However, the core heat-up and melting of the molten consolidated region continued, and the relocation of core material to the lower plenum occurred at 226 min. The water in lower plenum vaped which increase the pressure. After the block valve open, the forced circulation was restored and the core and molten pool in lower plenum cooled down slowly.

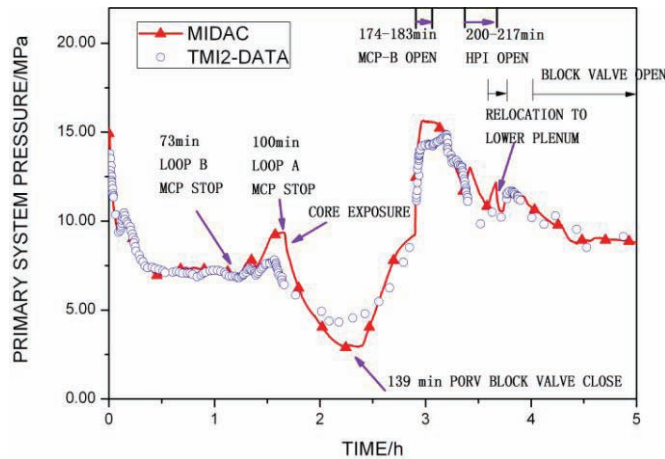


Figure 4. Variation of primary system pressure

The pressurizer water level is illustrated in Fig. 5. The MIDAC calculation result and the TMI-2 data are in good agreement for most of the accident progression. The difference increased after the loop A MCP shutting down and core exposure. The steaming rate and pressure in RPV decreased, leading to the decrease of water level in pressurizer. As the steam condensation in both A and B loop steam generator tubes were reduced by the hydrogen generated in the core, the pressurizer level remain relatively stable, until the loop 2B MCP restarted. The calculated value and the TMI-2 data increased after that due to the coolant entering the core and quickly evaporating. When the HPI started at 200min, the coolant inside the pressurizer discharged to the RPV, sharply reducing the pressurizer water level. After the block valve opening, the pressurizer was filled again.

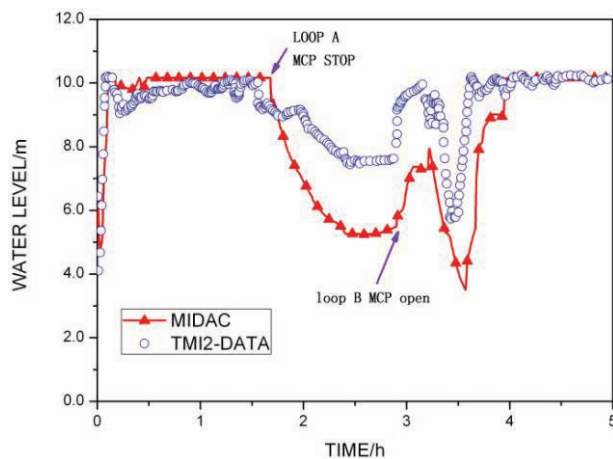


Figure 5. Variation of pressurizer water level

The mass flow rate of loop A and loop B in MIDAC calculation and TMI-2 data are presented in Fig. 6 and Fig. 7. The flow rate in reactor coolant loop includes not only the original inventory but also the operator controlled make up and letdown flows and the draining from the stuck-open PORV. As the boundary condition, the makeup and letdown flow rate were not quite clear due to the measure limitation in the TMI-2 accident. Furthermore, letdown, make-up and PORV flow rates are about 2 orders of magnitude less, and thus cannot be clearly appreciated in the comparison. The good agreement shown in the two figures reflects the accurate mass balance of the primary system in the simulation.

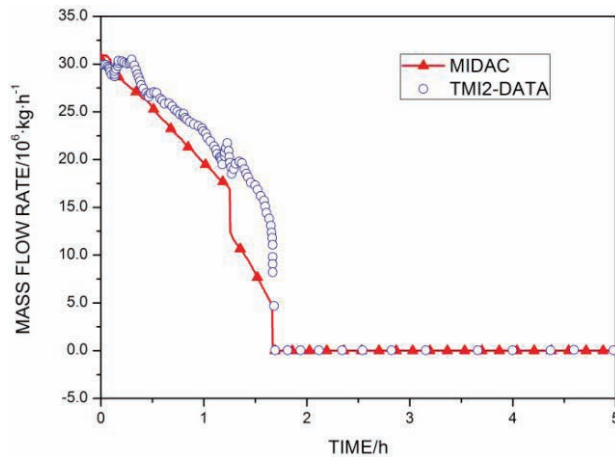


Figure 6. Mass flow rate in Loop A

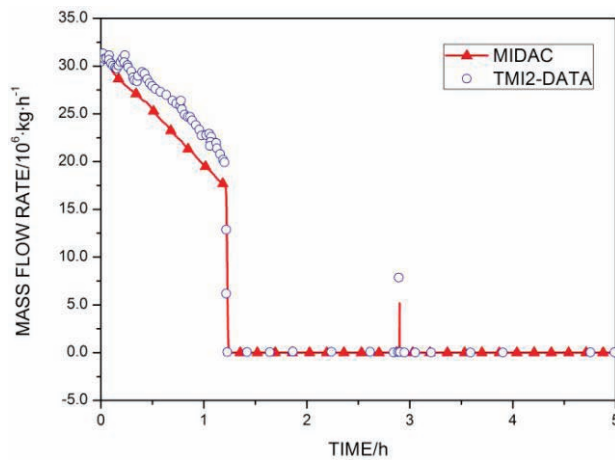


Figure 7. Mass flow rate in Loop B

The accumulated hydrogen production in the RPV is shown in the Fig. 8. The hydrogen generation started soon after the core uncovering and accelerated with the core heat-up process. About 395.8 kg hydrogen was produced before the loop 2B MCP restarted at 174 min. The production jumping after that was caused by the coolant reflooding the high temperature fuel cladding. The final production of hydrogen at the end of 5 h was 536.6 kg. The core material relocated into the lower head through the side crust of the molten pool at about 224 min. The total mass of debris in lower plenum is shown in Fig. 9. The mass of debris in the lower plenum is 14500 kg in the MIDAC simulation, while it is about 19000 kg in TMI-2 accident. The difference comes from various reasons. The mass of the molten materials and the damage core geometry are somewhat different with the real situation, in which many uncertainties are founded. The high temperature debris drained into the lower head, accumulating the debris bed that contacted with the lower head wall. The deformation of the wall or the crack in the molten pool crust can formed a thin gap between the debris and the wall. This kind of gap is significant for the cooling of the wall in contract with the debris. The temperature of the hot point in the lower head wall in contract with the debris is shown in Fig. 10. The node 1 to 5 represented the five layers of the wall from inner most to outer surface at the hot spot location. The gap size was insufficient for the cooling of the debris and the wall. Thus, the wall temperature increased sharply at the beginning of the relocation, which in turn increased the creep

deformation of the wall, causing the gap size increase. The temperature reached about 1050 °C for the inner most node, then decreased slowly for better cooling ability in the gap channel.

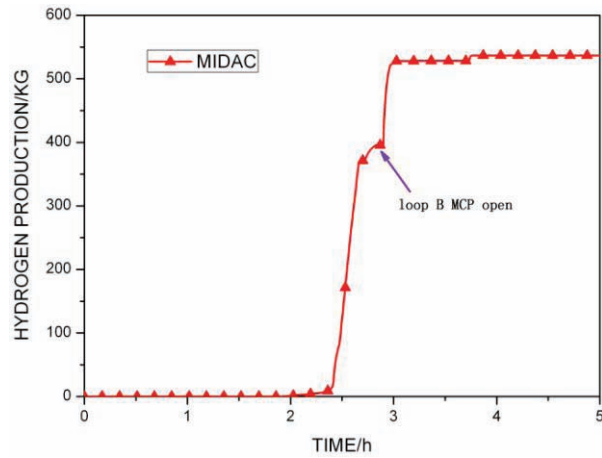


Figure 8. Accumulation hydrogen production

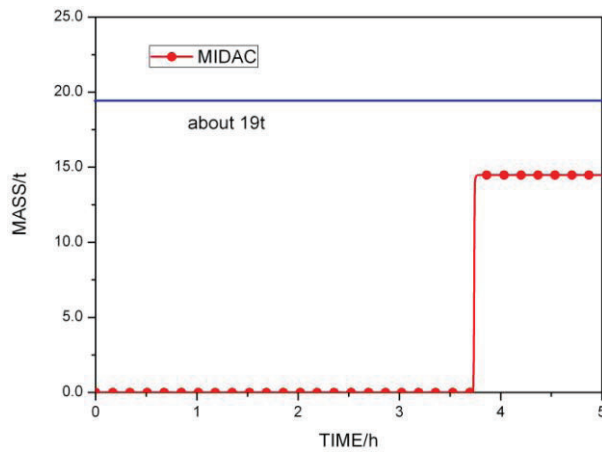


Figure 9. Mass of debris in lower plenum

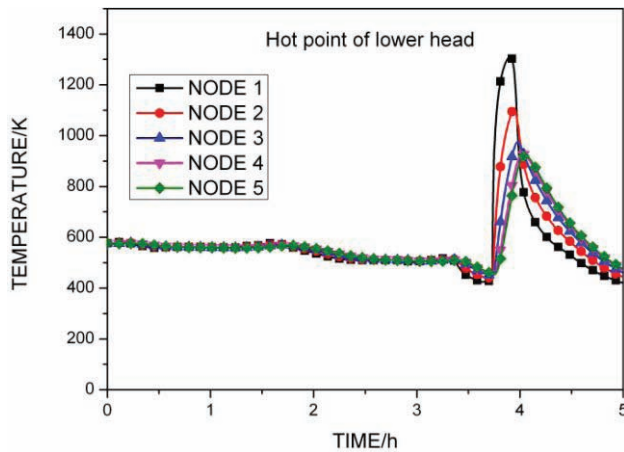


Figure 10. Wall temperature in the lower head

4. CONCLUSIONS

A module in-vessel core degradation analysis code MIDAC composed of five modules is developed in Xi'an Jiaotong University. The five modules, i.e., the core early behavior module, the core degradation module, the debris bed module, the RPV melt behavior module and the thermal hydraulic module are combined with each other and can simulate almost all the severe accident phenomena in the vessel. The former four modules related to severe accident are introduced in detail respectively. A code validation matrix is proposed based on the severe accident experiment research. As validation project, the TMI-2 accident, is introduced and conducted. The results show that the MIDAC code can well simulate the whole TMI-2 accident procession, and the calculated parameters agree well with the plant data.

ACKNOWLEDGMENTS

The authors appreciate the financial support from National Science and Technology Major Project (Grant Code: 2011ZX060 0 4-0 08).

REFERENCES

1. B.R. Sehgal, "Nuclear Safety in Light Water Reactor Safety". Chapter 1, 8, Academic Press, Boston, USA (2012).
2. W.C. Muller, "Review of Debris Bed Cooling in the TMI-2 Accident", *Nucl. Eng. Des.* 236(19-21), pp. 1965-1975(2006)
3. B.R. Sehgal, "Accomplishments and challenges of the severe accident research", *Nucl. Eng. Des.* 210(79), pp.79-94(2001)
4. L. Boshov, V. Strizhov, A. Kisselev, "Severe Accident Codes Status and Future Development" *Nucl. Eng. Des.* 173, pp. 247-256(1997)
5. J. Wang, W.X. Tian, Y.Q. Fan, , K.Y. Mao, J.N. Lu, G.H. Su, S.Z. Qiu, "The development of a zirconium oxidation calculating program module for module in-vessel degraded analysis code MIDAC", *Prog. Nucl. Energy* , **73**, pp. 162-171(2014).
6. K.I. Sugiyama, H. Aoki, G.H. Su, Y. kojima, "Experimental Study on Coolability of Particulate Core-Metal Debris Bed with Oxidization, (I) Fragmentation and Enhanced Heat Transfer in Zircaloy-50 wt% Ag Debris Bed", *J. Nucl. Sci. Technol.* **42**(12), pp.1081-1084(2005)
7. G.H. Su, K.I. Sugiyama, H. Aoki, I. Kimura, "Experiment study on coolability of particulate core-metal debris bed with oxidization, (II) fragmentation and enhanced heat Transfer in Zircaloy debris bed", *J. Nucl. Sci. Technol.* **43** (5), pp .537-545 (2006).
8. Y.P. Zhang, S.Z. Qiu, G.H. Su, W.X. Tian, "A simple novel analysis procedure for IVR calculation in core molten severe accident", *Nucl. Eng. Des.* **241**(12), 4634-4642(2011).
9. R.H. Chen, M. Corradini, G.H. Su, S.Z. Qiu, "Development of a solidification model for TEXASVI and application to FARO L14 analysis", *Nucl. Sci. Eng.* **173**, pp.1-10(2012).
10. L.Z. Li, Y.P. Zhang, S.Z. Qiu, G.H. Su, W.X. Tian, "MAAP5 simulation of the PWR severe accident induced by pressurizer safety valve stuck-open accident", *Prog. Nucl. Energy*, **77**, pp.141-151 (2014).
11. W. Li, et al. "Analysis of PWR RPV lower head SBLOCA scenarios with the failure of high-pressure injection system using MAAP5" *Prog. Nucl. Energy*, **77**, pp.48-64 (2014).
12. X.L. Wu, et al., "Analysis of the loss of pool cooling accident in a PWR spent fuel pool with MAAP5", *Ann. Nucl. Energy*, **72**, pp.198-213(2014).
13. L.Z. Li, et al., "Severe accident analysis for a typical PWR using the MELCOR code", *Prog. Nucl. Energy*, **71**, pp. 30-38(2014).
14. P. Hofmann, "Current knowledge on core degradation phenomena, a review", *J. Nucl. Mater.* **270**, pp.194-211(1999)

15. G. Schanz, B. Adroguer, A. Volchek, “Advanced treatment of zircalloy cladding high-temperature oxidation in SA code calculations Part I: experimental database and basic modeling”, *Nucl. Eng. Des.* **232**, pp.75–84 (2004).
16. X.W. Shi, X.R. Cao, Z.Z. Liu. “Oxidation behavior analysis of cladding during severe accidents with combined codes for Qinshan Phase II Nuclear Power Plant”, *Ann. Nucl. Energy*, **58**, pp.246-254 (2013).
17. A. Volchek, Yu. Zvonarev, G. Schanz, “Advanced treatment of zircalloy cladding high-temperature oxidation in SA code calculations PART II: best-fitted parabolic correlations”, *Nucl. Eng. Des.* **232**, pp. 85–96 (2004).
18. E. Beuzet, et al. “Modelling of Zry-4 cladding oxidation by air, under severe accident conditions using the MAAP4 code”, *Nucl. Eng. Des.* **241**, PP.1217-1224(2011).
19. I. Huhtiniemi, D. Magallon, H. Hohmann, “Results of recent KROTOS FCI tests: alumina versus corium melts”. *Nucl. Eng. Des.* **189**, pp. 379-389 (1998).
20. A. Karbojian, W.M. Ma, P. Kudinov, T.N. Dinh, “A scoping study of debris bed formation in the DEFOR test facility”, **239**, pp. 1653-1659(2009).
21. D. Magallon, “Characteristics of corium debris bed generated in large-scale fuel-coolant interaction experiments”. *Nucl. Eng. Des.* **236**, pp.1998-20 09(2006).
22. M. Salay, F. Fichot, “Modelling of Corium Stratification in the Lower Plenum of a Reactor Vessel”, *OECD/NEA MASCA Seminar 2004*, Aix-en-Provence, France, June 10-11, 2004.
23. “In-Vessel Core Degradation Code Validation Matrix-Update 1996-1999”, <http://www.oecd-nea.org/nsd/docs/2000/csni-r2000-21.pdf> (2000).
24. C.Y. Paik, R.E. Henry, M.A. McCartney, “MAAP4.0 benchmarking with the TMI-2 experience”. *International Conference on Probabilistic Safety Assessment Methodology and Applications*, Seoul, Korea, Nov. 26-30, 1995, pp.673-680.